Journal of Food Engineering 386 (2025) 112299

Contents lists available at ScienceDirect

Journal of Food Engineering

journal homepage: www.elsevier.com/locate/jfoodeng

Monitor and classify dough based on color image with deep learning

Bryan Gilbert Murengami [a], Xudong Jing [a], Hanhui Jiang [a], Xiaojuan Liu [a], Wulan Mao [a,d], Yuedan Li [e], Xueyong Chen [e,**], Shaojin Wang [a], Rui Li [a], Longsheng Fu [a,b,c,*]

[a] College of Mechanical and Electronic Engineering, Northwest A&F University, Yangling, Shaanxi, 712100, China
[b] Key Laboratory of Agricultural Internet of Things, Ministry of Agriculture and Rural Affairs, Yangling, Shaanxi, 712100, China
[c] Shaanxi Key Laboratory of Agricultural Information Perception and Intelligent Service, Yangling, Shaanxi, 712100, China
[d] Institute of Agricultural Mechanization, Xinjiang Academy of Agricultural Sciences, Urumqi, 830000, China
[e] College of Mechanical and Electrical Engineering, Fujian Agriculture and Forestry University, Fuzhou, 350001, China

ARTICLE INFO

Keywords:
Fermented dough
Dough monitoring
Optimal bread production
Ensemble learning

ABSTRACT

To address subjective, time-consuming, and labor-intensive manual methods for monitoring and classifying fermenting dough, an automated and non-destructive method is proposed. Deep learning model YOLOv8s and extracted features including dough surface area, contrast, and homogeneity from RGB color images were employed to monitor fermenting dough. The features were input to a stacked ensemble model (SEM) with base models SVM, AdaBoost, KNN, and RF, with AdaBoost as meta-learner to classify fermenting dough into under-fermented, fermented, and over-fermented. SEM demonstrated a high dough classification rate of 83%, with specific rates of 75% for under-fermented, 71% for fermented, and 90% for over-fermented dough. Results reviewed that combining dough surface area and texture features is effective for monitoring dough, and can be used in adjusting chamber conditions. Furthermore, SEM showed great ability in classifying fermenting dough. The proposed method offers a promising solution for improved bread quality and consistency in bread-making.

1. Introduction

Dough fermentation represents a pivotal phase in bread-making. Bread is one of the earliest "processed" foods made and consumed by humans and has nutritional value, offering carbohydrates, protein, dietary fiber, and antioxidants (Aghalari et al., 2022; Badaró et al., 2022; Cappelli et al., 2021). One key step in bread making is dough fermentation, which directly impacts final bread's quality, flavor, texture, and shelf life. Monitoring dough fermentation state enables modifying chamber conditions of dough fermentation (temperature and humidity) (Castro-Reigía et al., 2023). Meanwhile, determining fermenting dough readiness for baking is crucial; classifying doughs to under-fermented, fermented, and over-fermented can save time and energy (Castro-Reigía et al., 2023; Gally et al., 2017). Manual monitoring and classification of fermenting dough is subjective, time-consuming and labor-intensive, limiting ability to consistently produce high-quality bread (Chang et al., 2020; Giefer et al., 2019). Consequently, it is crucial for objective and automated methods to monitor and classify dough fermentation.

Area, volume and texture are important characteristics of fermenting dough and has been used to monitor and classify dough fermentation automatically. During dough fermentation, carbohydrates are converted into carbon dioxide and ethanol, forming gas bubbles resulting in dough area, volume, and texture changes. Volume is a significant indicator of dough fermentation (Giefer et al., 2019; Goetz et al., 2003; Nazeri et al., 2021; Soleimani Pour-Damanab et al., 2011; Zettel et al., 2016), because it directly reflects expansion of gas bubbles within dough, which are pivotal for monitoring and classifying dough (Bajd and Ser, 2011; Bonny et al., 2004; Ivorra et al., 2014; Romano et al., 2013, 2018; Shehzad et al., 2010). But measuring dough volume non-destructively is challenging. Area correlates with volume and has been explored to monitor dough fermentation (Ivorra et al., 2014; Verdú et al., 2015). In addition, texture offers a comprehensive assessment of fermenting dough, as it is linked to density and cellular structure, which is beneficial to monitor and classify dough fermentation (Della Valle et al., 2014; Ivorra et al., 2014). The current methods in bread-making are evasive, and others lack scalability for handling large samples (Bajd and Ser, 2011; Ivorra et al., 2014; Nazeri et al., 2021; Soleimani Pour-Damanab et al., 2011).

* Corresponding author. College of Mechanical and Electronic Engineering, Northwest A&F University, Yangling, Shaanxi, 712100, China.
** Corresponding author.
E-mail addresses: xueyongchen@fafu.edu.cn (X. Chen), fulsh@nwafu.edu.cn (L. Fu).

https://doi.org/10.1016/j.jfoodeng.2024.112299
Received 25 May 2024; Received in revised form 10 August 2024; Accepted 26 August 2024
Available online 28 August 2024
0260-8774/© 2024 Elsevier Ltd. All rights are reserved, including those for text and data mining, AI training, and similar technologies.



Fig. 1. A single batch of oval-shaped dough.

Therefore, it is essential to adopt a simple and practical method to obtain characteristics of fermenting dough.

RGB (Red, Green, and Blue) color imagery has great potential to provide characteristics of fermenting dough simply and non-destructively. Fermentation has been extensively studied by various imaging methods, including magnetic resonance imaging (MRI) (Bajd and Ser, 2011; Bonny et al., 2004; Goetz et al., 2003), X-ray (Babin et al., 2006, 2008; Turbin-Orger et al., 2012), near infra-red (NIR) (Castro-Reigía et al., 2023), structured light (SL) (Ivorra et al., 2014; Verdú et al., 2015), and RGB imaging (Romano et al., 2013; Soleimani Pour-Damanab et al., 2011; Zettel et al., 2016). Among them, RGB imaging has numerous advantages due to its non-invasiveness, cost-effectiveness, and simplicity (Ulrici et al., 2012). RGB images can provide characteristics of fermenting dough during dough fermentation, such as density (Soleimani Pour-Damanab et al., 2011) and volume (Zettel et al., 2016). Hence, RGB imaging is promising to monitor and classify fermenting dough state.

Continuous process of dough fermentation creates difficulties in monitoring and classifying dough automatically. Machine learning (ML) has potential to classify dough fermentation (Castro-Reigía et al., 2023). SEM is a promising ML algorithm for continuous processes as it enriches accuracy of individual predictions by combining models with distinct strengths and weaknesses (Jiang et al., 2023; Singh et al., 2020). Fermentation is influenced by numerous factors, leading to different states, depending on dough type. Flour is the main ingredient, and its fermentation characteristics varies (Chakrabarti-bell et al., 2021; Gally et al., 2017). This necessitates object detection and training individual models for each dough type, especially in industrial bread-making. You Only Look Once version eight small (YOLOv8s) is a cutting-edge object detection network with exceptional speed. It has been integrated into online detection tasks, for rapid detection, similar to dough detection (Li et al., 2023; H. Zhao et al., 2024). In this study an automated method using RGB imaging and machine vision is developed to address manual fermenting dough monitoring and classification. The method leveraged YOLOv8s for dough type detection, and monitoring. Subsequently, features, including surface area, contrast, homogeneity, corelation and energy, are extracted. These features are then fed into SEM to classify dough state.

2. Materials and methods

2.1. Dough preparation

In this study, an automatic dough monitoring and classification method is proposed. Six dough types were selected, namely: oval-shaped, focaccia, circle, puff, bagel, and bean-shaped. Among them, oval-shaped type was randomly selected to validate the proposed method. Oval-shaped dough was prepared using 250 g flour (Wonder Farm, Cangzhou, China), 2 g yeast (Meishan, Zhengzhou, China), 4 g salt, 10 g caster sugar, and water. After mixing, dough was rested for 10 min at room temperature. Each day, the dough was shaped to make at least two batches of four identical oval-shaped samples, as shown in Fig. 1. The shaped dough was rested for 5 min, then fermented with temperatures between 27 °C and 31 °C under 75% and 80% relative

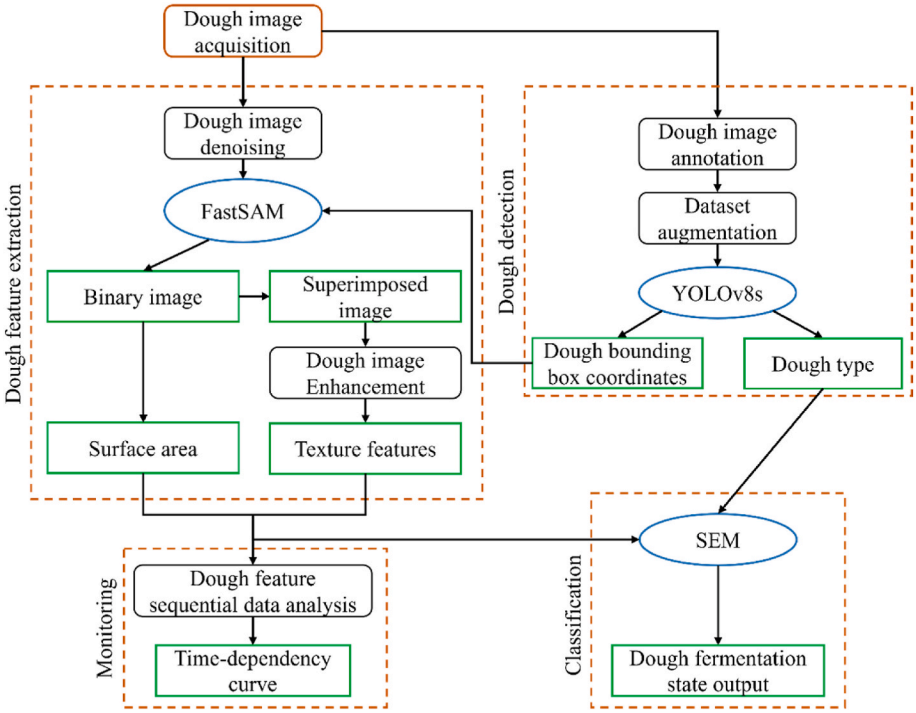


Fig. 2. The proposed pipeline. Orange color depicts the stages, while black rectangles represent operations, and the green ones are outputs of either an operation or a model. The blue ellipse represents the models.

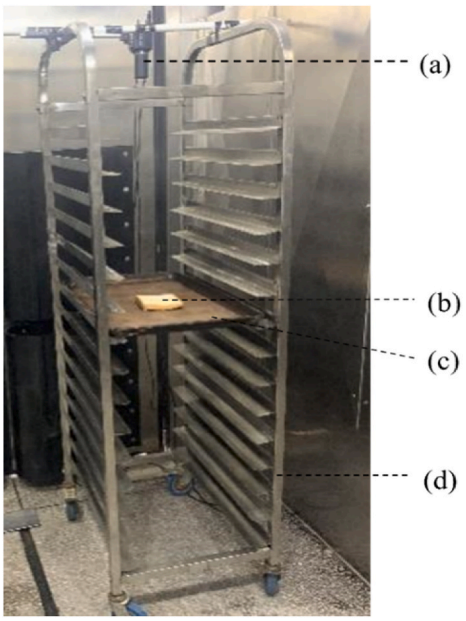


Fig. 3. Image acquisition platform for dough, including (a) camera, (b) dough sample, (c) tray, and (d) trolley.

humidity. Since dough was identical, four doughs in an image were assumed to exhibit same fermentation state. Fermentation was done 13 times on four separate days, at least twice each day, totaling 52 dough samples.

2.2. Proposed pipeline

The proposed method comprises five stages, depicted in Fig. 2. In the first stage, fermenting dough RGB images are captured by a camera. The acquisition process is different for the following two stages, i.e., feature extraction and dough detection. Images are detected for dough type and bounding box coordinates using YOLOv8s in stage two. Third stage, dough surface area (DSA) and texture features are extracted, and a segmentation model uses bounding box coordinates of detected dough as input. In stage four, fermenting dough is monitored by tracking features, and in stage five, the features are input to SEM for classification.

2.3. Image acquisition

The experiments were conducted in Longyan (Fujian Province, China) in 2022 and 2023. Images were acquired for two distinct purposes: feature extraction and dough detection. Image acquisition platform is shown in Fig. 3. The platform is a bread trolley (dimensions: 820 × 690 × 1620 mm) which can hold up to 14 trays of dough. The bread trolley was inside a dark stainless steel fermentation chamber with controlled temperatures and humidity. An industrial camera (SUA1201C, Mindvision, Shenzhen, China) and a LED (QLED3-105-1C, Yueting Lighting, Shangqiu, Henan Province, China) were mounted atop the trolley. The camera features a 4000 × 3000-pixel resolution, 32 fps maximum frame, 0 °C – 50 °C operating temperature, and 20%–80% operating humidity. The LED provided consistent illumination inside the dark chamber to enhance image capture quality. A black tray was chosen as the background to improve contrast with the light-colored dough samples. The background color is essential as it influences dough detection and segmentation, thus a black color increases contrast between dough sample and background (Soleimani Pour-Damanab et al., 2011). Calibration was performed for lighting, focal length, aperture, camera position, and dough sample placement to ensure clear and complete capture of dough images.

During acquisition for feature extraction five trays were removed from the trolley top to and oval-shaped dough samples were placed on a tray 50 cm below the camera, as shown in Fig. 3. Images were acquired at 30 s intervals. In total 465 images were collected and subsequently classified by an experienced baker panel into under-fermented (236

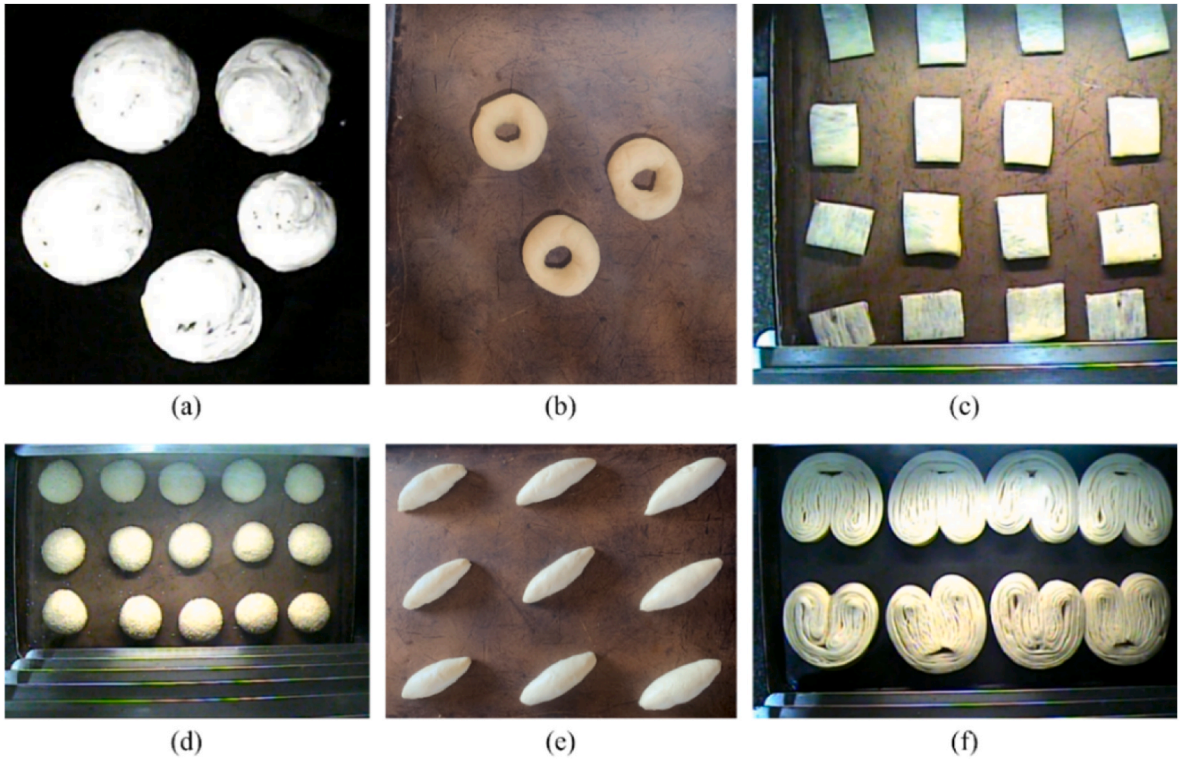


Fig. 4. Dough samples of (a) circle, (b) bagel, (c) focaccia, (d) puff, (e) oval-shaped, and (f) bean-shaped.

images), fermented (125 images), and over-fermented (104 images). The feature extraction dataset comprised of 440 images and was partitioned into a training set and a validation set in a 5:1 ratio. The training set contained 366 images (198 under-fermented, 97 fermented, and 71 over-fermented), while the validation set consisted of 74 images. The validation set had, 30 under-fermented, 21 fermented, and 23 over-fermented images. The remaining 25 images were used to evaluate the proposed method. This evaluation dataset had (8 under-fermented, 7 fermented, and 10 over-fermented) images.

Image acquisition platform for dough detection was the same, but dough images of six different types were acquired since dough type influences fermentation (Chakrabarti-bell et al., 2021; Gally et al., 2017). The images were acquired at varying distances to enhance the models' robustness to object size variations and each type had a different number of doughs (2–36) per tray as shown in Fig. 4.

2.4. Dough detection

YOLOv8s was employed for dough detection. The dough detection training dataset had a total of 2965 images: oval-shaped (546), focaccia (498), circle (678), puff (197), bagel (488), and bean-shaped (597), samples are shown in Fig. 4. Images were labeled with rectangular boxes using LabelImg software (https://github.com/tzutalin/labelImg). Data augmentation techniques, including horizontal flip, rotation, brightness, and mosaic, were implemented to increase number of training images from 2965 to 6200. The dataset was partitioned into training set (4340 images), validation set (1240 images), and testing set (620 images). The trained network was then used to identify dough images, providing both a bounding box and specific dough type. Subsequently, the segmentation model utilized bounding box coordinates and dough type was used to load trained weights of SEM.

2.5. Fermenting dough feature extraction

Accurate estimation of DSA, and texture is crucial for automated dough monitoring and classification. During acquisition, image quality can be affected by noises like white noise and pretzel noise. Hence, a median filter was used to denoise dough images using Eq. (1). The filter replaces each pixel in the image with median value of its neighboring pixels (Barbin et al., 2016).

$$\widehat{f}(x,y) = median_{(s,t)\in S_{xy}}\{g(s,t)\} \tag{1}$$

where S_{xy} are coordinates of sub-image of window size 5 × 5.

2.5.1. DSA estimation

In previously described method for surface area estimation (Sabliov et al., 2002) the segmentation technique employed demonstrated sensitivity to noise, posed challenges in determining a threshold value, and susceptible to interference from reflections or shadows. Therefore, this study used fast segment anything (FastSAM) (https://github.com/CASIA-IVA-Lab/FastSAM) (X. Zhao et al., 2023). The input parameters of FastSAM were *img_size* of 640, *conf* of 0.45, and *IoU* of 0.5, and bounding box coordinates supplied by YOLOv8s. The model outputs a binary image, which is used in estimating DSA by Eq. (2).

$$A = \sum_{i=1}^{n} A_i = \sum_{i=1}^{n} \frac{\pi}{2}(D_i + D_j)\sqrt{\left(\frac{D_j}{2} - \frac{D_i}{2}\right)^2 + dh^2} \tag{2}$$

where, D_i and D_j are diameters, n is the number of frustums and dh is height of frustrum.

To ensure accuracy and reliability of estimated DSA, 13 doughs were measured manually by placing a scale at the bottom of the tray near the dough. The dimensions of dough were obtained just before fermentation. Simultaneously, images were captured from a top view, and Mindvision measuring software was utilized to convert dimensions to pixels for computing conversion factors. This step was necessary to obtain true DSA. The dough appeared as an ellipsoid from top view, and DSA was determined by Eq. (3).

$$D_{area} = \pi \times a \times b \tag{3}$$

where a represents length of semi-major axis and b represents length of semi-minor axis.

2.5.2. Texture feature extraction

Texture features were extracted from a superimposed image. The output of FastSAM, a binary image, was superimposed onto original image, with white pixels identifying dough and black pixels representing background. This facilitated analysis of region of interest by eliminating interference from tray reflections, or bread clumps. Then adaptive histogram equalization was implemented to enhance superimposed images using an 8 × 8 tile grid size. Haralick texture features, namely contrast, homogeneity, energy and correlation, were extracted from enhanced superimposed image to quantify spatial relationships within the dough microstructure (Haralick RM, 1973). These texture features were chosen as they are known to be sensitive to variations in dough porosity (Della Valle et al., 2014; Jian and Wang, 2019). The features were calculated using Eq. (4), (5), (6), and (7), a distance of 2 pixels and four angles (0°, 45°, 90°, and 135°). Recursive feature elimination (RFE), a wrapper method was employed for feature selection (Xu et al., 2022).

$$Contrast = \sum_{i=1}^{n}\sum_{j=1}^{n}(1-j)^2 p_\theta(i,j) \tag{4}$$

$$Homogeneity = \sum_{i=1}^{n}\sum_{j=1}^{n} p_\theta(i,j)^2 \tag{5}$$

$$Energy = \sum_{i=1}^{n}\sum_{j=1}^{n} p_\theta(i,j)\log(p_\theta(i,j)) \tag{6}$$

$$Correlation = \sum_{i=0}^{n-1}\sum_{i=0}^{n-1}\frac{p_\theta(i,j)\left[(i-\mu_x)\left(i-\mu_y\right)\right]}{\delta x \delta y} \tag{7}$$

where, p (i, j) is the gray-level co-occurrence matrix element at pixel (i, j).

2.6. Fermenting dough monitoring

Oval-shaped dough was monitored by tracking DSA and texture features. Sequential data of area and texture features were recorded at 30-s intervals, allowing for direct observation of changes during fermentation. Time-dependent curves (TDC) were generated to visualize changes in each feature and assess any correlations with expert baker observations. By monitoring these features, fermentation process can be understood. For instance, changes in dough area provide insights into the expansion and growth of dough. Texture offers valuable information about the dough's consistency and structure. Contrast and homogeneity evaluations help assess uniformity and distribution of components within the dough, while energy indicate metabolic activity. Therefore, this monitoring approach can provide a comprehensive understanding of dough fermentation, which is vital in classifying its fermentation state.

2.7. Fermenting dough classification

SEM was applied to classify dough fermentation state. Ensemble techniques, such as bagging, boosting, and stacking, have been successfully used in various classification challenges (Dutta et al., 2015; Xu et al., 2022). Among them, stacking has shown good performance across different problems. A typical SEM consists of one or more layers. The

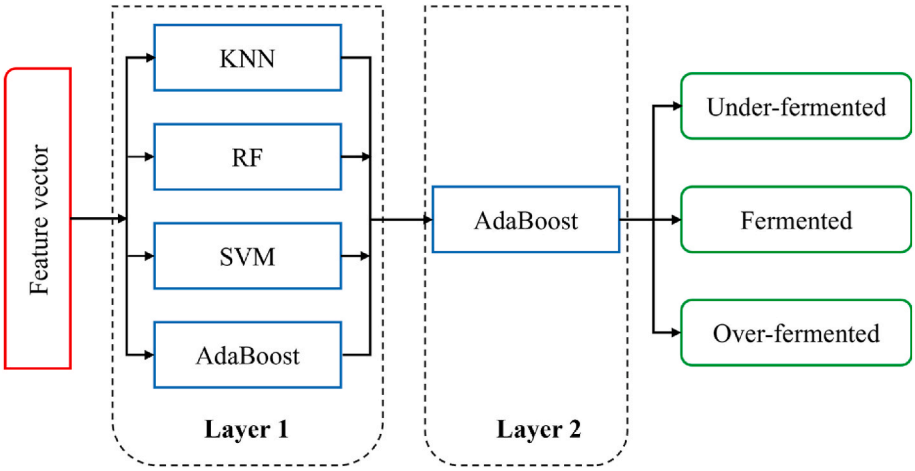


Fig. 5. SEM structure. Red rectangles represent input feature vector, blue represent SEM models and green are outputs. The feature vector is input into BMs and the output is fed to meta-learner which classifies dough.

Table 1
Training parameters of YOLOv8s.

Parameters	Learning rate	Momentum	Weight decay	Batch size	Epochs
Value	0.01	0.937	0.0005	4	120

Table 2
SEM optimal hyperparameters obtained by GridSearchCV.

Models	Hyperparameter space
XGBoost	learning_rate = 0.1, max_depth = 3
SVM	C = 1.0, kernel = rbf, gamma = 0.1
DT	max_depth = 20, min_samples_split = 10
AdaBoost	n_estimators = 50, learning_rate = 0.1
NB	alpha = 1.0, force_alpha = warn
GBDT	learning_rate = 0.1, max_depth = 2
KNN	n_neighbors = 10, leaf_size = 10
LR	solver = lbfgs, C = 0.1, max_itr = 1000
RF	n_estimators = 100, max_depth = 5

first layer called base layer, includes one or several ML models known as base models (BMs), while the second layer's models is a meta-learner.

Selection of BMs and meta-learner plays a crucial role in the performance of SEM (Jiang et al., 2023). However, there is no fixed method for selecting BMs, as studies report different combinations. In this study, nine models were selected as candidate BMs, including XGBoost, Support Vector Machine (SVM), Logistic Regression (LR), Random Forest (RF), Decision Tree (DT), K-Nearest Neighbors (KNN), AdaBoost, Gradient Boosting Decision Tree (GBDT), and Naïve Bayes (NB). These models are well-known for their accuracy, speed, and robustness to outliers. A step-by-step approach described in (Xu et al., 2022) was followed for BMs selection. Fig. 5 provides a summarized description of stacking approach, which can be outlined in the following three steps:

S1. Train individual BMs M_{bN} given a training dough dataset $D = \{(x_i, y_i)\}_{i=1}^{k}$ sliced into 5 folds where $x_i \in R^n$, $y_i \in R^n$ are input and output data points respectively.

S2. Construct a new dataset $D' = \{(x'_i, y'_i)\}_{i=1}^{k}$, where $x'_i = [M_{b1}(x_i), M_{b2}(x_i), \ldots M_{bN}(x_i)]$ and $y'_i = y_i$.

S3. Train meta-learner M_{meta} on new dataset D' return $M\{M_{b1}(x), M_{b2}(x) \ldots M_{bN}(x)\}$ and this model will be used to make predictions on new data points by combining predictions of base models.

2.8. Training setting

YOLOv8s network training was conducted in a computer with AMD Ryzen 7 5800X 8-Core Processor CPU, Nvidia GeForce GTX 3080 Ti 12 GB GPU, and 64 GB of memory. While SEM was trained on an ASUS Intel Core i7-7700HQ processor with an NVIDIA GeForce GTX1650, with both machines operating on Windows 10 system. Training hyperparameters for YOLOv8s are shown in Table 1, while those of SEM are presented in Table 2.

2.9. Evaluation metrics

Evaluation indicators, i.e., *precision (P)*, *recall (R)*, $F1_{\text{score}}$ and *mAP* score were used to evaluate SEM and YOLOv8s. *P* evaluates detection result relevancy, and *R* measures relevant detection results. *P* and *R*, are defined by Eq. (8), and Eq. (9), respectively. For dough in an image, when correctly detected it is true positive (*TP*), false negative (*FN*) if wrongly detected and false positive (*FP*) if detected but not labeled. $F1_{\text{score}}$ defined in Eq. (10) is a blend of *P* and *R*. The *mAP* (mean average precision) was adopted to evaluate YOLOv8s, defined by Eq. (11). SEM was evaluated using *dough classification rate* (*DCR*) defined in Eq. (12) (*N* is 25 images classified by experienced panel).

$$P = \frac{TP}{TP + FP} \tag{8}$$

$$R = \frac{TP}{TP + FN} \tag{9}$$

$$F1_{score} = \frac{2P \times R}{P + R} \tag{10}$$

$$mAP = \frac{1}{n}\sum_{i=0}^{n} AP_i \tag{11}$$

$$DCR = \frac{TP}{N} \times 100\% \tag{12}$$

where *n* is number of instances in dataset, and *y* is true label.

Performance of DSA extraction method was evaluated using several metrics: *rooted mean squared error* (*RMSE*), *mean, minimum* (*min*), *maximum* (*max*) and *standard deviation* (*STDEV*) (Du and Sun, 2006; Sabliov et al., 2002). The error was defined as percentage difference between manually measured and estimated DSA.

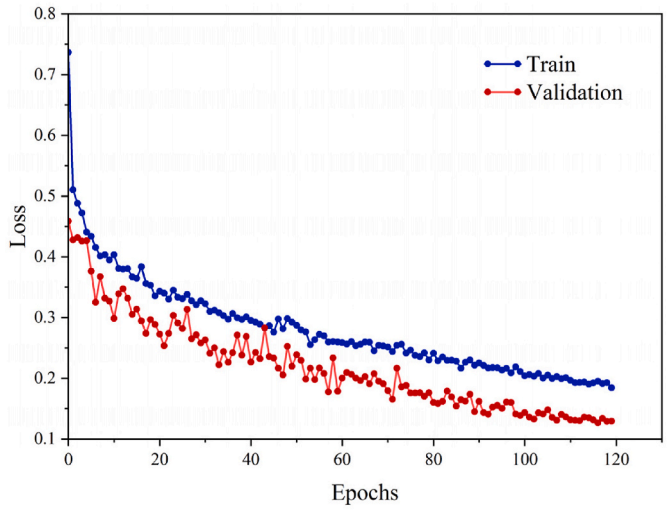


Fig. 6. YOLOv8s model training and validation performance loss curve.

3. Results and discussion

3.1. YOLOv8s for dough detection

YOLOv8s is suitable for detecting fermenting dough. During training, YOLOv8s model exhibited a steady decrease in loss, reaching 0.23 within 80 epochs, indicating efficient feature extraction, as depicted in Fig. 6. After 115 epochs, the loss plateaued around 0.19, suggesting convergence. On the other hand, validation loss rapidly declined to below 0.2 within 60 epochs and stabilized around 0.13 by epoch 107. This behavior demonstrates the model's ability to generalize without overfitting, further supported by high *P* and *R* of 99% and *mAP* of 98%.

The excellent performance of YOLOv8s can be attributed to three key factors, transfer learning, distinct dough shapes and, data augmentation, as suggested in previous studies (Jian and Wang, 2019). The trained model was evaluated several times, to ensure its robustness. During experiments the model detected dough with confidence averaging 90% as shown in Fig. 7. It was observed that when oval-shaped dough was left to ferment for a longer time, its shape increasingly became similar to circle-shaped type as shown by Fig. 7c. However, the model could detect dough type accurately, although bounding box would overlap in such instances.

3.2. Fermenting dough monitoring

3.2.1. Evaluation of DSA estimation method

The proposed method can be used to estimate DSA. Table 3 presents comparison results of proposed method with manually measured DSA. Results show that the proposed method exhibited both underestimation and overestimation of DSA, as indicated by min error of −6% and max error of 4%. However, *mean* error, representing average of max and min errors, indicates that the method performs reasonably well. Furthermore, the lower *mean* error compared to *STDEV* indicates consistent performance of proposed method. The low *RMSE* of 0.98 cm^2 shown by Fig. 8 further supports the accuracy of the proposed method in estimating DSA.

3.2.2. Fermenting DSA analysis

DSA has previously been used to monitor dough (Verdú et al., 2015). TDC offer valuable insights into the dynamics of dough fermentation, hence serves as a good tool for monitoring fermentation. Fig. 9 presents TDC for dough's estimated DSA. The oval-shaped dough exhibited rapid increase in DSA between 0 and 20 min, followed by a gradual slowdown. From 40 min, DSA increased much slower. DSA changes observed remained consistent across three days, however, on day_2, the curve was slightly lower. This variance could be due to differences in initial size of oval-shaped dough. It is important to highlight that this variation does not impact the monitoring of the dough. However, it does emphasize the importance of maintaining a consistent dough size during the preparation process.

Table 3
Comparison of manual and proposed method estimating fermenting DSA.

	Area (cm^2)		Error (%)
	Manual	Proposed method	
Mean	26.30	26.13	−0.50
Min	21.41	22.05	−6.20
Max	29.05	30.35	4.49
STDEV	2.56	2.25	4.03

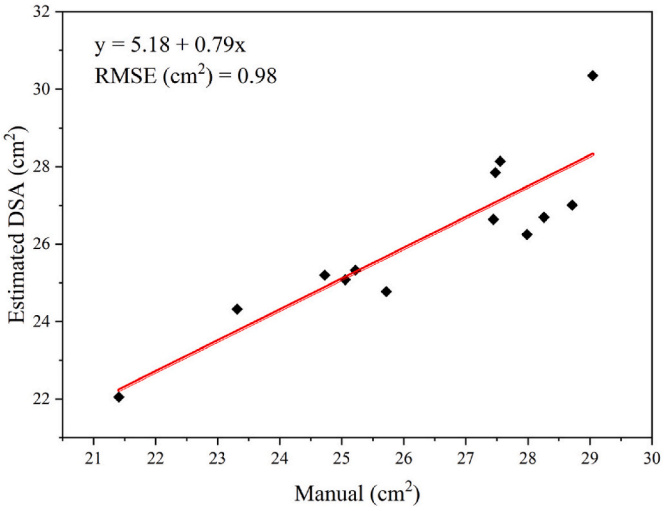


Fig. 8. Performance of the proposed method for estimating DSA vs manual method.

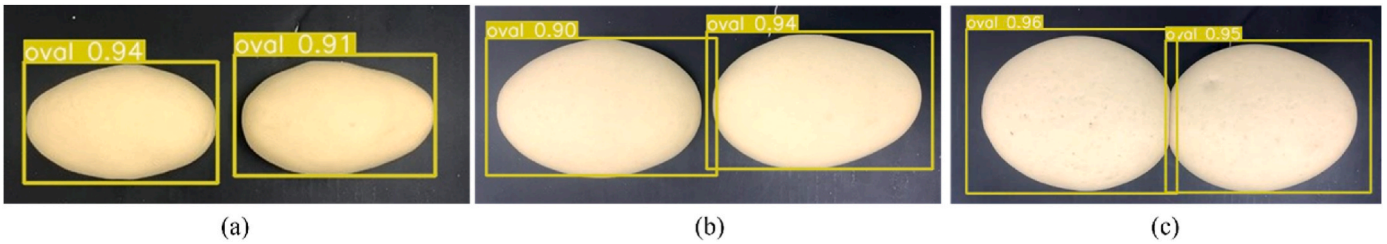


Fig. 7. YOLOv8s dough detection. Initial detection of under-fermented dough (a), detection of same dough after 25 min (b), and detection after 50 min with shape resembling circle type and overlapping bounding boxes (c).

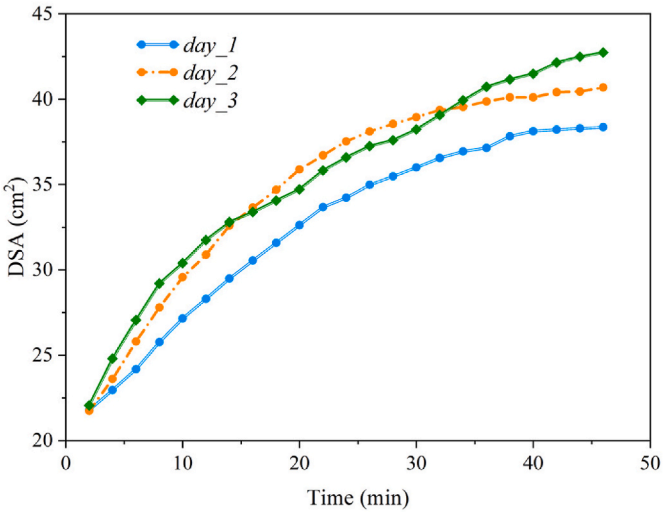


Fig. 9. DSA changes during fermentation on three different days. DSA curve for day_2 is slightly lower than other two days, but overall pattern remains consistent.

3.2.3. Analysis of texture features

Texture features, homogeneity and contrast are suitable for monitoring dough fermentation. Previous research has not explored utilizing texture features for monitoring fermenting dough, but dough undergoes visible surface changes during fermentation as shown in Fig. 10. Therefore, four texture features were extracted, and RFE was used to rank key features, eliminating energy and correlation. TDC were plotted with homogeneity and contrast representing the ordinate and time on the abscissa. As shown in Fig. 11a, oval-shaped fermenting dough loses uniformity as fermentation progresses, consistently observed over three days. Additionally, contrast of dough increases significantly during fermentation, depicted in Fig. 11b. Notably, on *day_2*, an irregular curve is observed, indicating an issue with the setup in the fermentation chamber.

Analysis indicates that DSA and texture features exhibited clear changes that allows monitoring using TDC. Texture can be used to replicate baker experience in monitoring fermenting dough. For instance, as depicted in Figs. 10 and 11, the visual changes on dough surface, typically relied upon by experienced bakers for dough monitoring corresponds to specific texture values. Hence, combining DSA and texture features can provide a robust method for monitoring dough and obtaining information that can be used to adjust chamber conditions.

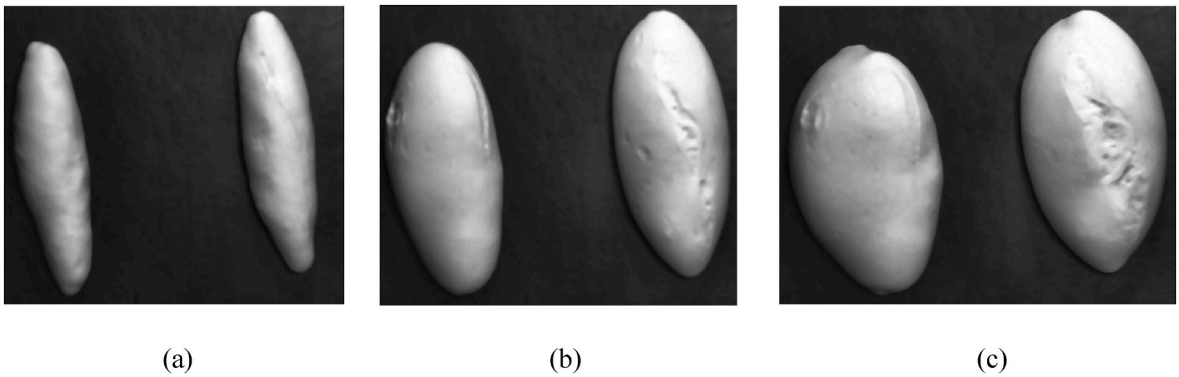


Fig. 10. Visual assessment of dough fermentation. (a) Oval-shaped dough captured 2 min after fermentation initiation exhibits a smooth surface. (b) After 25 min, dough retains perfect oval shape. (c) Following 45 min of fermentation, the surface becomes rough and uneven.

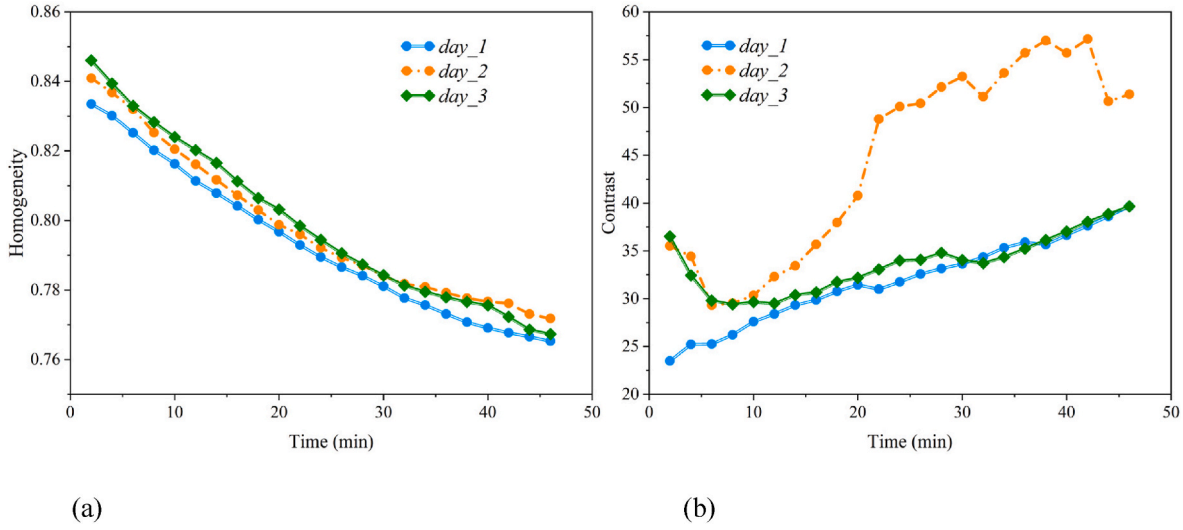


Fig. 11. Texture changes during fermentation. (a) Dough texture loses homogeneity. (b) Contrast on dough surface increases. Irregular curve on *day_2* suggests an issue with fermentation chamber setup.

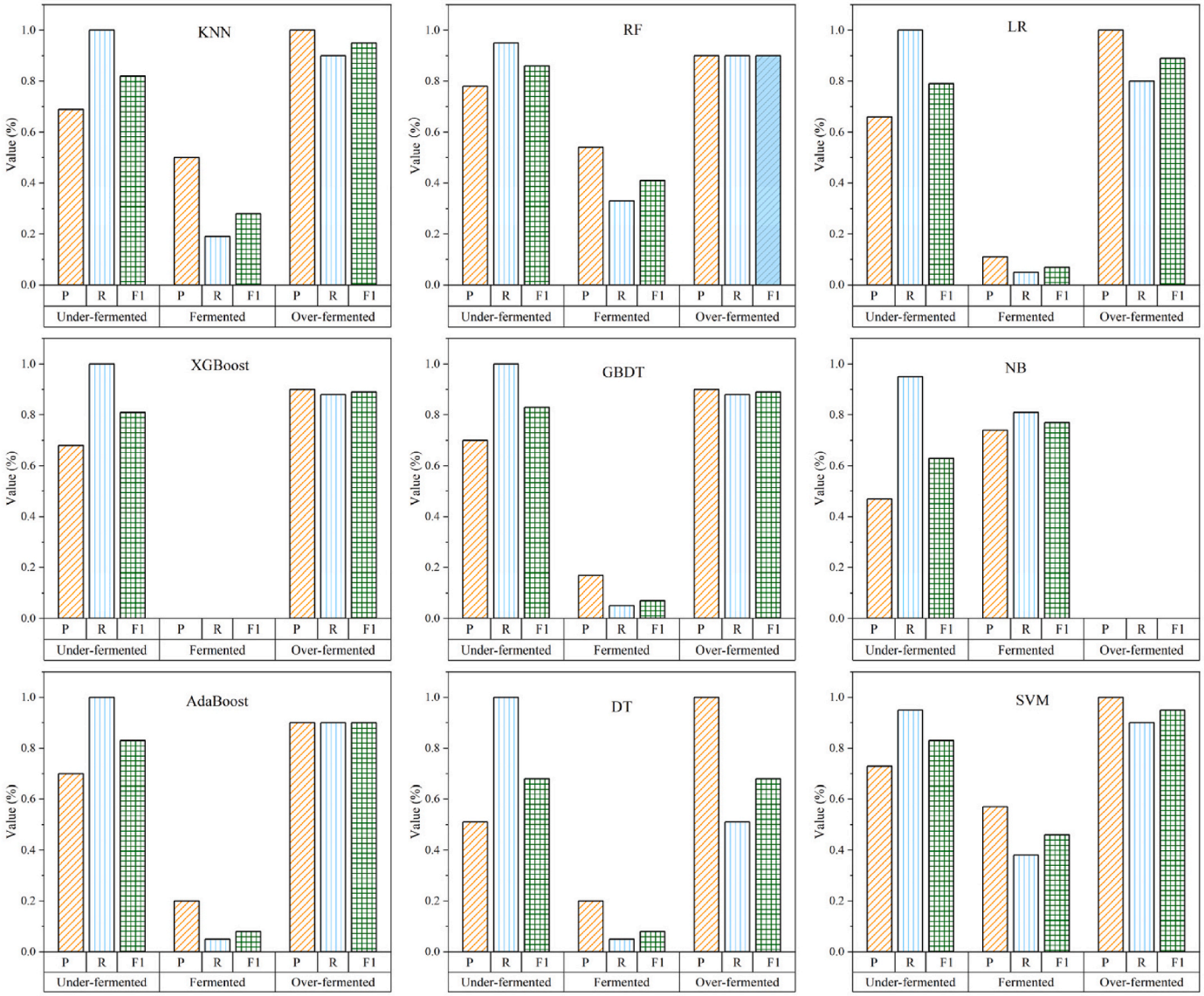


Fig. 12. Fermenting dough classification performance of nine candidate base models for three classes.

3.3. Fermenting dough classification

3.3.1. BMs selection

Accuracy and diversity are valuable indicators when selecting BMs for a SEM. Nine models were employed to classify dough, and results are presented in Fig. 12. Performance evaluation of each model on specific classes revealed that RF, SVM, GBDT, and AdaBoost demonstrated superiority in identifying under-fermented dough. RF demonstrated exceptional performance in identifying under-fermented dough with *P* above 75%. Models faced difficulties classifying fermented dough, with eight obtaining *P* and *R* below 60%, except NB. XGBoost was poor in this regard, failing to classify any fermented dough. Despite NB's good performance in classifying fermented dough, it failed to identify any over-fermented samples. Most models achieved high *P* and *R* above 80% for over-fermented, except NB and DT.

The models performed well in classifying under-fermented and over-fermented dough. However, faced challenges in identifying fermented dough, which could be attributed to the continuous nature of fermentation process. The inconsistency with NB suggests that it assumed that all the dough belonged to the fermented class.

Finally, XGBoost, SVM, AdaBoost, GBDT, KNN, and RF achieved $F1_{score}$ above 80% for under-fermented dough. The low $F1_{score}$ for fermented dough indicate poor performance in this category, while for over-fermented, models performed well with $F1_{score}$ above 80%. Although NB showed potential in identifying fermenting dough, its contribution cannot be relied upon. Based on this assessment, SVM, RF, KNN, and AdaBoost were selected as candidate BMs.

3.3.2. Meta-learner selection and classification performance

The choice of meta-learner model plays a significant role in the overall accuracy of the SEM. The impact of varying BMs on classification accuracy is shown in Fig. 13. SEM using two BMs outperformed candidate BMs. Performance further improved with three BMs and a RF meta-learner, shown in Fig. 13b. Highest metrics were achieved using four BMs and AdaBoost as the meta-learner, shown in Fig. 13c, demonstrating that increasing number of BMs enhances SEM accuracy (Jiang et al., 2023). *P* for under-fermented, fermented, and over-fermented dough were above 80%, while *R* was above 70%. $F1_{score}$ was above 75%, indicating a strong agreement between *P* and *R*. Based on these metrics, SVM, RF, KNN, and AdaBoost were selected to construct SEM.

The SEM model demonstrates effective classification of fermenting dough. In comparison to other ensemble methods, SEM outperformed them in terms of *P*, *R*, and $F1_{score}$, as shown in Table 4. For under-fermented SEM achieved $F1_{score}$ of 9% better than blending ensemble

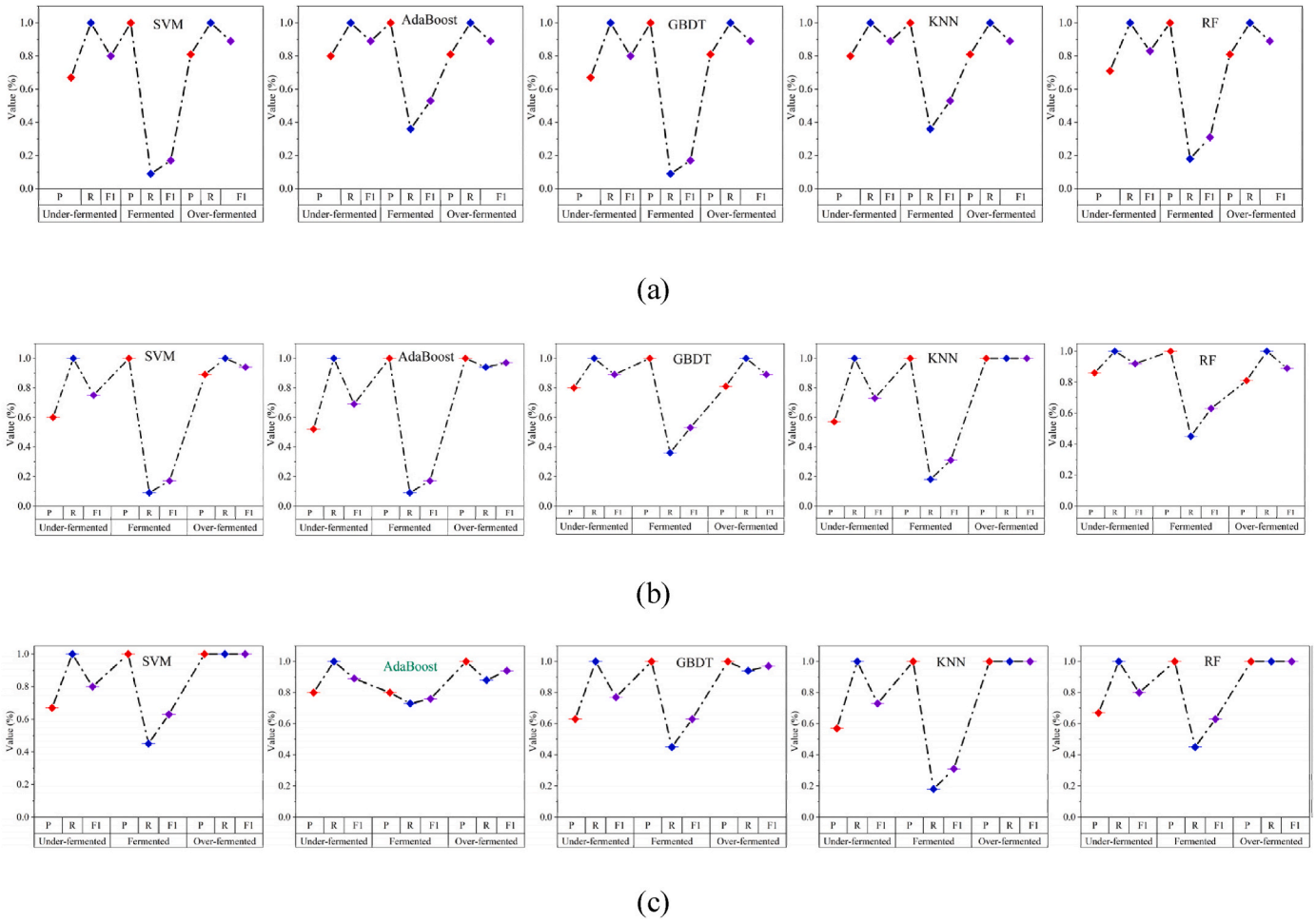


Fig. 13. Classification performance of stacked combinations of, (a) two, (b) three and (c) four BMs candidates with different meta-learners for the three classes.

Table 4
Classification performance comparison SEM, BEM and VEM.

Methods	Base models	Under-fermented			Fermented			Over-fermented		
		Precision	Recall	$F1_{score}$	Precision	Recall	$F1_{score}$	Precision	Recall	$F1_{score}$
SEM	KNN, SVM, AdaBoost, RF	**0.80**	**1.00**	**0.89**	**0.80**	**0.73**	**0.76**	**1.00**	**0.88**	**0.94**
BEM	KNN, SVM, AdaBoost, RF	0.67	1.00	0.80	0.29	0.45	0.36	1.00	0.29	0.45
VEM	AdaBoost, RF	0.71	1.00	0.83	1.00	0.18	0.31	0.81	1.00	0.89
	SVM, AdaBoost, RF	0.67	1.00	0.80	1.00	0.09	0.17	0.81	1.00	0.89
	KNN, SVM, AdaBoost, RF	0.55	1.00	0.71	1.00	0.09	0.17	1.00	1.00	1.00

Note: AdaBoost is meta-leaner, overall best metrics marked in bold.

model (BEM) and 6% better than voting ensemble model (VEM). The improvement is consistent for fermented and over-fermented. Results also indicate that increasing base models in VEM did not improve performance compared to SEM. The superiority of SEM over BEM and VEM has been reported in several studies (Chaudhary et al., 2016; Xu et al., 2022). Fig. 14 further demonstrates the performance of SEM compared to BMs. Additionally, SEM obtained higher *R* compared to Castro-Reigía et al. (2023), who got *R* of 88%, 86%, and 86% for under-fermented, fermented, and over-fermented doughs, respectively. These findings highlight effectiveness of SEM for identifying fermenting dough.

3.3.3. *Evaluation of the proposed method*

The proposed method can be used for automatic monitoring and classification of fermenting dough in industrial bread-making. To assess the viability of this method in monitoring and classifying fermenting dough, a set of 25 images underwent manual classification by a panel, categorizing them into under-fermented, fermented and over-fermented dough classes. Subsequently, each image was fed into the YOLOv8s model at 30-s intervals for dough type detection, followed by segmentation using FastSAM. The process continued with the extraction of DSA and texture features (contrast, and homogeneity) to monitor each fermenting dough sample. The fermenting dough state in each RGB image was obtained by leveraging a pretrained SEM model. Noteworthy is the efficiency of this workflow, all these steps completed within 0.77 s per image. In terms of SEM performance evaluation, the model exhibited a DCR of 83%, with class-specific DCRs of 75%, 71%, and 90% for under-fermented, fermented, and over-fermented dough, respectively. The relatively lower DCR observed for fermented dough can be attributed to the continuous nature of the fermentation process.

Nevertheless, the method indicates its effectiveness in monitoring and classifying fermenting dough. Previous works have been limited to monitoring fermenting dough without classification and often used

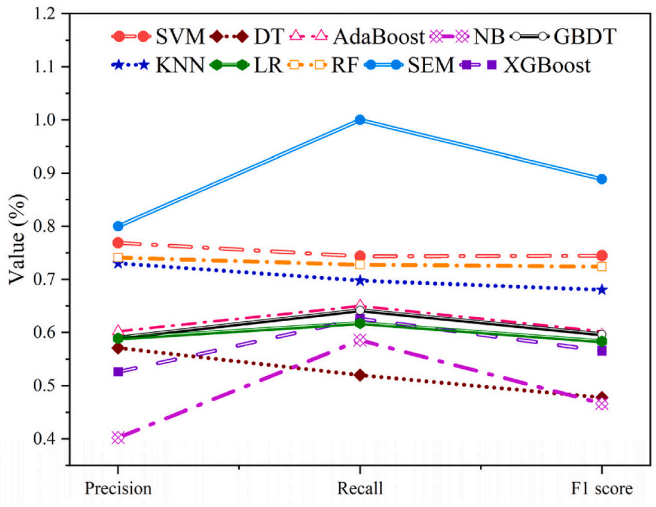


Fig. 14. Classification performance of SEM and BMs.

expensive or destructive methods (Castro-Reigía et al., 2023; Ivorra et al., 2014; Nazeri et al., 2021), thus this approach is effective.

4. Conclusions

This study presents an automatic, non-destructive method for monitoring and classifying fermenting dough into under-fermented, fermented, and over-fermented. By utilizing YOLOv8s and RGB imaging, the method successfully tracks changes in surface area and texture during fermentation. The analysis of dough surface area, contrast, and homogeneity provides valuable insights into the evolution of dough. The classification accuracy achieved by SEM is high, indicating its effectiveness in accurately categorizing dough. Accuracy, diversity, and number of base models should be considered when constructing an SEM. In this work, SEM has four base models (SVM, RF, KNN, and AdaBoost) and AdaBoost as the meta-learner. The proposed method can be used in automating dough fermentation monitoring and classification. Future research directions involve exploring the application of deep-learning models to further enhance accuracy and reliability.

CRediT authorship contribution statement

Bryan Gilbert Murengami: Writing – original draft, Software, Methodology, Conceptualization. **Xudong Jing:** Data curation, Software. **Hanhui Jiang:** Writing – review & editing, Validation, Methodology, Conceptualization. **Xiaojuan Liu:** Validation, Methodology, Conceptualization. **Wulan Mao:** Visualization, Methodology. **Yuedan Li:** Software, Investigation, Data curation. **Xueyong Chen:** Writing – review & editing, Supervision, Methodology. **Shaojin Wang:** Writing – review & editing, Conceptualization. **Rui Li:** Writing – review & editing, Conceptualization. **Longsheng Fu:** Writing – review & editing, Supervision, Conceptualization.

Declaration of competing interest

The authors declare that they have no known competing financial interests.

Data availability

Data will be made available on request.

Acknowledgements

This work was supported by the National Natural Science Foundation of China (32171897) ;National Foreign Expert Project, Ministry of Science and Technology, China (DL2022172003L, QN2022172006L), Zhangzhou Golden Key Machinery Co., Ltd. (107/KH200064A).

References

Aghalari, Z., Dahms, H.U., Sillanpää, M., 2022. Evaluation of nutrients in bread: a systematic review. J. Health Popul. Nutr. 41 (1), 41. https://doi.org/10.1186/s41043-022-00329-3.

Babin, P., Della Valle, G., Chiron, H., Cloetens, P., Hoszowska, J., Pernot, P., Réguerre, A. L., Salvo, L., Dendievel, R., 2006. Fast X-ray tomography analysis of bubble growth and foam setting during breadmaking. J. Cereal. Sci. 43 (3), 393–397. https://doi.org/10.1016/j.jcs.2005.12.002.

Babin, P., Della Valle, G.D., Chiron, H., Cloetens, P., Hoszowska, J., Pernot, P., Réguerre, A.L., Salvo, L., Dendievel, R., 2008. In situ fast X-ray tomography study of the evolution of cellular structure in bread dough during proving and baking. Bubbles in Food 2: Novelty, Health and Luxury 7, 265–272. https://doi.org/10.1016/B978-1-891127-59-5.50030-4.

Badaró, A.T., Hebling e Tavares, J.P., Blasco, J., Aleixos-Borrás, N., Barbin, D.F., 2022. Near infrared techniques applied to analysis of wheat-based products: recent advances and future trends. Food Control 140. https://doi.org/10.1016/j.foodcont.2022.109115.

Bajd, F., Ser, I., 2011. Continuous monitoring of dough fermentation and bread baking by magnetic resonance microscopy. Magn. Reson. Imag. 29, 434–442. https://doi.org/10.1016/j.mri.2010.10.010.

Barbin, D.F., Mastelini, S.M., Barbon, S., Campos, G.F.C., Barbon, A.P.A.C., Shimokomaki, M., 2016. Digital image analyses as an alternative tool for chicken quality assessment. Biosyst. Eng. 144, 85–93. https://doi.org/10.1016/j.biosystemseng.2016.01.015.

Bonny, J.M., Rouille, J., Della Valle, G., Devaux, M.F., Douliez, J.P., Renou, J.P., 2004. Dynamic magnetic resonance microscopy of flour dough fermentation. Magn. Reson. Imag. 22 (3), 395–401. https://doi.org/10.1016/j.mri.2004.01.020.

Cappelli, A., Lupori, L., Cini, E., 2021. Baking technology: a systematic review of machines and plants and their effect on final products, including improvement strategies. Trends Food Sci. Technol. 115, 275–284. https://doi.org/10.1016/j.tifs.2021.06.048.

Castro-Reigía, D., García, I., Sanllorente, S., Sarabia, L.A., Amigo, J.M., Ortiz, M.C., 2023. Bread fermentation monitoring through NIR spectroscopy and PLS-DA. Determining the optimal fermentation point in bread doughs. J. Food Eng. 361, 111738 https://doi.org/10.1016/j.jfoodeng.2023.111738.

Chakrabarti-bell, S., Lukasczyk, J., Liu, J., Maciejewski, R., Xiao, X., Mayo, S., Regenauer-lieb, K., 2021. Flour quality effects on percolation of gas bubbles in wheat flour doughs. Innovative Food Sci. Emerging Technol. 74, 102841 https://doi.org/10.1016/j.ifset.2021.102841.

Chang, X., Huang, X., Tian, X., Wang, C., Aheto, J.H., Ernest, B., Yi, R., 2020. Dynamic characteristics of dough during the fermentation process of Chinese steamed bread. Food Chem. 312, 126050 https://doi.org/10.1016/j.foodchem.2019.126050.

Chaudhary, A., Kolhe, S., Kamal, R., 2016. A hybrid ensemble for classification in multiclass datasets: an application to oilseed disease dataset. Comput. Electron. Agric. 124, 65–72. https://doi.org/10.1016/j.compag.2016.03.026.

Della Valle, G., Chiron, H., Cicerelli, L., Kansou, K., Katina, K., Ndiaye, A., Whitworth, M., Poutanen, K., 2014. Basic knowledge models for the design of bread texture. Trends Food Sci. Technol. 36 (1), 5–14. https://doi.org/10.1016/j.tifs.2014.01.003.

Du, C.J., Sun, D.W., 2006. Estimating the surface area and volume of ellipsoidal ham using computer vision. J. Food Eng. 73 (3), 260–268. https://doi.org/10.1016/j.jfoodeng.2005.01.029.

Dutta, R., Smith, D., Rawnsley, R., Bishop-Hurley, G., Hills, J., Timms, G., Henry, D., 2015. Dynamic cattle behavioural classification using supervised ensemble classifiers. Comput. Electron. Agric. 111, 18–28. https://doi.org/10.1016/j.compag.2014.12.002.

Gally, T., Rouaud, O., Jury, V., Havet, M., Ogé, A., Le-bail, A., 2017. Proofing of bread dough assisted by ohmic heating. Innovative Food Sci. Emerging Technol. 39, 55–62. https://doi.org/10.1016/j.ifset.2016.11.008.

Giefer, L.A., Lütjen, M., Rohde, A.K., Freitag, M., 2019. Determination of the optimal state of dough fermentation in bread production by using optical sensors and deep learning. Appl. Sci. 9 (20) https://doi.org/10.3390/app9204266.

Goetz, J., Groß, D., Koehler, P., 2003. On-line observation of dough fermentation by magnetic resonance imaging and volumetric measurements. Eur. Food Res. Technol. 217 (6), 504–511. https://doi.org/10.1007/s00217-003-0796-y.

Haralick RM, S.K., 1973. Textural features for image classification. EEE Transactions on Systems, Man, and Cybernetics 3, 610–621.

Ivorra, E., Verdú, S., Sánchez, A.J., Barat, J.M., Grau, R., 2014. Continuous monitoring of bread dough fermentation using a 3d vision structured light technique. J. Food Eng. 130, 8–13. https://doi.org/10.1016/j.jfoodeng.2013.12.031.

Jian, G.Z., Wang, C.M., 2019. The bread recognition system with logistic regression. In: Communications in Computer and Information Science. Springer, Singapore. https://doi.org/10.1007/978-981-13-9190-3_14. Vol. 1013, Issue 57.

Jiang, H., Zhang, S., Yang, Z., Zhao, L., Zhou, Y., Zhou, D., 2023. Quality classification of stored wheat based on evidence reasoning rule and stacking ensemble learning. Comput. Electron. Agric. 214, 108339 https://doi.org/10.1016/j.compag.2023.108339.

Li, P., Zheng, J., Li, P., Long, H., Li, M., Gao, L., 2023. Tomato maturity detection and counting model based on MHSA-YOLOv8. Sensors 23 (15), 6701. https://doi.org/10.3390/s23156701.

Nazeri, F.S., Kadivar, M., Izadi, I., 2021. A sensing system for continuous monitoring of bread dough during fermentation. Sensing and Imaging 22 (1), 14. https://doi.org/10.1007/s11220-021-00337-3.

Romano, A., Campagna, R., Masi, P., Cuomo, S., Toraldo, G., 2018. Data-driven approaches to predict states in a food technology case study. In: IEEE 4th International Forum on Research and Technologies for Society and Industry, RTSI 2018 - Proceedings. https://doi.org/10.1109/RTSI.2018.8548426 v, 5.

Romano, A., Cavella, S., Toraldo, G., Masi, P., 2013. 2D structural imaging study of bubble evolution during leavening. Food Res. Int. 50 (1), 324–329. https://doi.org/10.1016/j.foodres.2012.10.040.

Sabliov, C.M., Boldor, D., Keener, K.M., Farkas, B.E., 2002. Image processing method to determine surface area and volume of axi-symmetric agricultural products. Int. J. Food Prop. 5 (3), 641–653. https://doi.org/10.1081/JFP-120015498.

Shehzad, A., Chiron, H., Della Valle, G., Kansou, K., Ndiaye, A., Réguerre, A.L., 2010. Porosity and stability of bread dough during proofing determined by video image analysis for different compositions and mixing conditions. Food Res. Int. 43 (8), 1999–2005. https://doi.org/10.1016/j.foodres.2010.05.019.

Singh, S.K., Vidyarthi, S.K., Tiwari, R., 2020. Machine learnt image processing to predict weight and size of rice kernels. J. Food Eng. 274, 109828 https://doi.org/10.1016/j.jfoodeng.2019.109828.

Soleimani Pour-Damanab, A.R., Jafary, A., Rafiee, S., 2011. Monitoring the dynamic density of dough during fermentation using digital imaging method. J. Food Eng. 107 (1), 8–13. https://doi.org/10.1016/j.jfoodeng.2011.06.010.

Turbin-Orger, A., Boller, E., Chaunier, L., Chiron, H., Della Valle, G., Réguerre, A.L., 2012. Kinetics of bubble growth in wheat flour dough during proofing studied by computed X-ray micro-tomography. J. Cereal. Sci. 56 (3), 676–683. https://doi.org/10.1016/j.jcs.2012.08.008.

Ulrici, A., Foca, G., Cristina, M., Antonella, L., Pietro, D., Fiego, L., 2012. Automated identification and visualization of food defects using RGB imaging : application to the detection of red skin defect of raw hams. Innovative Food Sci. Emerging Technol. 16, 417–426. https://doi.org/10.1016/j.ifset.2012.09.008.

Verdú, S., Ivorra, E., Sánchez, A.J., Barat, J.M., Grau, R., 2015. Relationship between fermentation behavior, measured with a 3D vision structured light technique, and the internal structure of bread. J. Food Eng. 146, 227–233. https://doi.org/10.1016/j.jfoodeng.2014.08.014.

Xu, C., Ding, J., Qiao, Y., Zhang, L., 2022. Tomato disease and pest diagnosis method based on the stacking of prescription data. Comput. Electron. Agric. 197 (17), 106997 https://doi.org/10.1016/j.compag.2022.106997.

Zettel, V., Paquet-Durand, O., Hecker, F., Hitzmann, B., 2016. Image analysis and mathematical modelling for the supervision of the dough fermentation process. In: AIP Conference Proceedings. https://doi.org/10.1063/1.4963606, 1769.

Zhao, H., Cui, H., Qu, K., Zhu, J., Li, H., Cui, Z., Wu, Y., 2024. A fish appetite assessment method based on improved ByteTrack and spatiotemporal graph convolutional network. Biosyst. Eng. 240, 46–55. https://doi.org/10.1016/j.biosystemseng.2024.02.011.

Zhao, X., Ding, W., An, Y., Du, Y., Yu, T., Li, M., Tang, M., Wang, J., 2023. Fast segment anything. ArXiv 2. https://doi.org/10.48550/arXiv.2306.12156.